# Hadro- and photo-production of $\eta'$ in quasi-free proton and neutron processes*

HUANG Fei(黄飞)[1;1)] K. Nakayama[1,2;2)]

1 (Department of Physics and Astronomy, University of Georgia, Athens, GA 30602, USA)
2 (Institut für Kernphysik and Jülich Center for Hadron Physics, Forschungszentrum Jülich, D-52425 Jülich, Germany)

**Abstract** The $\eta'$ photoproduction process on quasi-free proton and neutron and the reaction $NN \to \eta' NN$ are investigated within a relativistic effective Lagrangian approach to hadronic interactions. Resonances with spins 1/2 and 3/2 are considered together with the nucleonic and $t$-channel meson-exchange current contributions. In photoproduction processes, the $S_{11}$ resonance is found to be responsible for the sharp rise of the cross sections near threshold. In $pp \to \eta' pp$, it is found that the $S_{11}$ resonance dominates the total cross section over the entire energy region considered. The spin observables, in particular the beam and target asymmetries, are shown to be very sensitive to the reaction mechanism and will help impose more stringent constraints on the model parameters.

**Key words** $\eta'$ production, free and quasi-free photoproduction, meson production in NN collisions

**PACS** 25.20.Lj, 13.60.Le, 25.24.-h

## 1 Introduction

One of the primary motivations for studying the production of mesons off nucleons is to investigate the structure and properties of nucleon resonances and, in the case of heavy-meson productions, to learn about hadron dynamics at short range. In particular, a clear understanding of the production mechanisms of mesons heavier than the pion still requires further theoretical and experimental investigation. Apart from pion production, the majority of theoretical investigations of meson-production processes are performed within phenomenological meson-exchange approaches. Such approaches force us to correlate as many independent processes as possible within a single model if one wishes to extract meaningful physics information. Indeed, this is the basic motivation behind the coupled-channel approaches. Here we present some selected results of our investigation of $\eta'$-meson production in the reactions $\gamma N \to \eta' N$ and $NN \to \eta' NN$ based on a relativistic meson-exchange approach.

A particular interest in investigating the $\eta'$ production reactions is that it may be suited to extract information on nucleon resonances, $N^*$, in the less explored higher $N^*$ mass region. Current knowledge of most of the nucleon resonances is mainly due to the study of $\pi N$ scattering and/or pion photoproduction off the nucleon. Since the $\eta'$ meson is much heavier than a pion, $\eta'$ meson-production processes near threshold necessarily sample a much higher resonance-mass region than the corresponding pion production processes. Therefore, in addition to serving as isospin filter, they are well-suited for investigating high-mass resonances in low partial-wave states. Furthermore, reaction processes such as $\eta'$ photoproduction provide opportunities to study those resonances that couple only weakly to pions, in particular, those referred to as "missing resonances", which are predicted by quark models, but not found in more traditional pion-production reactions[1].

Another special interest in $\eta'$ production off nucleon is the possibility to impose a more stringent constraint on its yet poorly known coupling strength

Received 7 August 2009
* Supported by FFE-COSY (41788390)
1) E-mail: huang@physast.uga.edu
2) E-mail: nakayama@uga.edu

to the nucleon. This has attracted much attention in connection with the so-called "nucleon-spin crisis" in polarized deep inelastic lepton scattering[2]. In the zero-squared-momentum limit, the $NN\eta'$ coupling constant $g_{NN\eta'}(q^2=0)$ is related to the flavor-singlet axial charge $G_A$ through the flavor singlet Goldberger–Treiman relation[3] (Refs. [4—6])

$$2m_N G_A(0) = F g_{NN\eta'}(0) + \frac{F^2}{2N_F} m_{\eta'}^2 g_{NNG}(0) \ , \quad (1)$$

where $F$ is a renormalization-group invariant decay constant defined in Ref. [3][1)], $N_F$ is the number of flavors, and $m_N$ and $m_{\eta'}$ are the nucleon and $\eta'$ masses, respectively; $g_{NNG}$ describes the coupling of the nucleon to the gluons arising from contributions violating the Okubo-Zweig-Iizuka (OZI) rule[7]. The EMC collaboration[2] has measured an unexpectedly small value of $G_A(0) \approx 0.20 \pm 0.35$; a more recent analysis of the SMC collaboration[8] yields a comparable value of $G_A(0) \approx 0.16 \pm 0.10$. The first term on the right-hand side of the above equation corresponds to the quark contribution to the "spin" of the proton, and the second term to the gluon contribution[5, 9]. Therefore, once $g_{NN\eta'}(0)$ is known, Eq. (1) may be used to extract the coupling $g_{NNG}(0)$. Unfortunately, however, there is no direct experimental measurement of $g_{NN\eta'}(0)$ so far. Reaction processes where the $\eta'$ meson is produced directly off a nucleon may thus offer a unique opportunity to extract this coupling constant. Here it should be emphasized that hadronic model calculations such as the present one cannot determine the $NN\eta'$ coupling constant in a model-independent way. At best, we get an estimate for the range of its value at the on-shell kinematic point, i.e., at $q^2 = m_{\eta'}^2$. Assuming the usual behavior of hadronic form factors for off-shell mesons which generally decrease for $q^2 < m^2$, we expect then that an eventually small upper limit of $g_{NN\eta'}(q^2 = m_{\eta'}^2)$ would lead to an even smaller value of $g_{NN\eta'}(0)$, which is needed in Eq. (1) to extract $g_{NNG}(0)$.

In contrast to lighter pseudoscalar $\pi$ and $\eta$ meson productions, not many data existed until quite recently for the $\eta'$ meson production reactions. Indeed, in photoproduction, only the earlier total cross section data from the ABBHHM Collaboration[10] were available until the late 1990s. More recently, the differential cross section data from the SAPHIR[11] and the CLAS[12] Collaborations – the latter of high-precision quality – became available. Currently, the beam asymmetry in this reaction is being measured by the CLAS Collaboration. The CBELSA/TAPS Collaboration has now reported measurements of cross sections in $\eta'$ photoproduction on both quasi-free proton and neutron (see I. Jaegle's talk in this meeting[13]). Also, data from the LEPS Collaboration (see T. Nakano's talk in this meeting[14]) will soon become available. For $NN \to NN\eta'$, there are data for total cross sections for excess energies up to $Q \approx 150$ MeV and for the differential cross sections at two excess energies[15]. Also, the pp and $p\eta'$ invariant mass distribution data have been reported by the COSY-11 Collaboration[16]. In addition, data for $pn \to pn\eta'$ will be available soon also from the COSY-11 Collaboration[17]. The addition of these new data has increased the database for $\eta'$ production considerably and should help make more detailed investigation of this meson production processes than in the past.

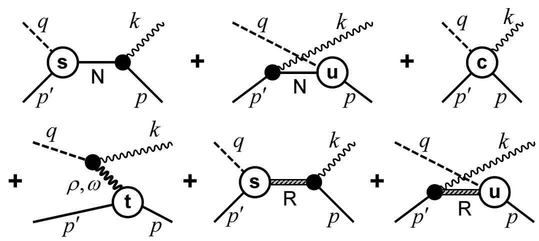


Fig. 1. Diagrams contributing to $\gamma p \to \eta' p$. Time proceeds from right to left. The intermediate baryon states are denoted N for the nucleon, and R for the nucleon resonances. The intermediate mesons in the $t$-channel are $\rho$ and $\omega$. The external legs are labeled by the four-momenta of the respective particles and the labels s, u, and t of the hadronic vertices correspond to the off-shell Mandelstam variables of the respective intermediate particles. The three diagrams in the lower part of the diagram are transverse individually; the three diagrams in the upper part are made gauge-invariant by an appropriate choice (see text) of the contact current depicted in the top-right diagram. The nucleonic current (nuc) referred to in the text corresponds to the top line of diagrams; the meson-exchange current (mec) and resonance current contributions correspond, respectively, to the leftmost diagram and the two diagrams on the right of the bottom line of diagrams.

In view of the considerable increase in the $\eta'$ meson production database as mentioned above, in the present work we revisit this meson production in photon- and nucleon-induced reactions. We describe these reactions in the following manner: the photoproduction reaction is calculated by considering the

1) In the OZI limit, $F = \sqrt{2N_F} F_\pi$, where $F_\pi$ stands for the pion decay constant.

s-, u- and t-channel Feynman diagrams plus a generalized contact term[18], which ensures gauge invariance of the total amplitude, in addition to accounting for the final-state interaction (FSI) effects. (See Ref. [19] for details.) The resulting dynamical content of the photoproduction amplitude is illustrated in Fig. 1.

The calculations of the photoproduction reaction on quasi-free proton and neutron are performed by simply folding the corresponding cross section on the free nucleon with the momentum distribution of the nucleon inside the deuteron.

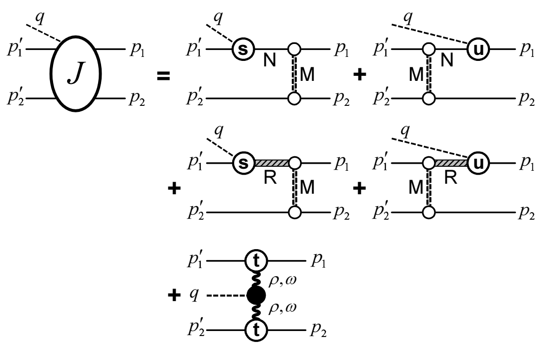

Fig. 2. Basic production mechanisms for NN → η′NN. Time proceeds from right to left. The full amplitude, with additional initial- and final-state contributions, is given by Eq. (2). As in Fig. 1, N and R denote the intermediate nucleon and resonances, respectively, and M incorporates all exchanges of mesons π, η, ρ, ω, σ, and $a_0$ (≡ δ) for the nucleon graphs and π, ρ, and ω for the resonance graphs. External legs are labeled by the four-momenta of the respective particles; the hadronic vertices s, u, and t here correspond to the same kinematic situations, respectively, as those identified similarly in Fig. 1. The nucleonic, resonance, and meson-exchange contributions referred to in the text correspond, respectively, to the first, second, and third lines of the diagrams on the right-hand side.

The NN → η′NN process is calculated in the Distorted-Wave Born Approximation (DWBA), where both the NN FSI and the initial-state interaction (ISI) are taken into account explicitly. The reaction amplitude is then given by

$$M=(1+T_fG_f)J(1+G_iT_i)\ , \tag{2}$$

where $T_\alpha$ denotes the NN ISI and FSI as $\alpha=i$ and $f$; $G_\alpha$ stands for the corresponding NN propagator. $J$ denotes the basic production amplitude. The NN FSI is known to be responsible for the dominant energy dependence observed in the total cross section (apart from the dependence due to the phase space) arising from the very strong interaction in the S-wave states at very low energies. As for the basic meson-production amplitude $J$ in Eq. (2), our model [18, 20] includes the nucleonic, mesonic, and nucleon resonance currents which are derived from the relevant effective Lagrangians. It is illustrated in Fig. 2.

The free parameters of our model — the resonance parameters, the NNM coupling constant, and the cutoff parameter $\Lambda_v^*$ at the electromagnetic vector-meson exchange vertex — are fixed such as to reproduce the available data in a global fitting procedure of the reaction processes considered in this work. The details of the present approach are fully described in Refs. [18, 20].

## 2 Results

In the following sections we present a few selected results for η′ photoproduction on quasi-free proton and neutron as well as for the η′ production in NN collisions.

### 2.1 η′ photoproduction on quasi-free proton and neutron

In the present calculation of the η′ photoproduction on quasi-free proton there are no free parameters to adjust, since all the relevant ones have been fixed[18] from the CLAS data for photoproduction on free proton[12]. The parameter set corresponding to that of Table 1 of Ref. [18] is used in this work. It includes the following resonances: $S_{11}(1958)$, $P_{11}(2104)$, $P_{13}(1885)$, and $D_{13}(1823)$. In addition, we have introduced an extra resonance with a mass of about 2.2 GeV. As discussed in connection to Fig. 3 below for the total cross section, this is required to reproduce the (preliminary) angular distribution data on quasi-free neutron from the CBELSA/TAPS Collaboration[13]. Other parameter sets yield similar results. Our predictions agree nicely with the (preliminary) angular distribution data from the CBELSA/TAPS Collaboration[13] for the entire measured angular and energy ranges. For η′ photoproduction on the quasi-free neutron, we have the Rnγ coupling constants as free parameters. They have been adjusted to fit the (preliminary) data from the CBELSA/TAPS Collaboration[13]. The fit quality is good with $\chi^2/N\sim1.2$.

Figure 3 shows our predictions for the total cross sections in η′ photoproduction on both the quasi-free proton (upper panel) and neutron (lower panel). We also show the corresponding results for the free proton and neutron cases. First, it is interesting to note that the little bump structure predicted for free proton case at around 2.1 GeV washes out completely in the quasi-free proton case. Similar feature is also seen in the neutron target case. The only difference here is that the bump structure is strong enough in the free case that it still survives in the quasi-free case after the folding with the neutron momentum distribution in the deuteron. This illustrates that weak resonances may not be seen in quasi-free processes which might have been revealed in free processes. Now, comparing the quasi-free proton and neutron cases, we see that in the quasi-free proton case no bump structure is present, while in the quasi-free neutron case, we see a bump structure around 2.2 GeV. In the present case, this structure arises from the extra resonance with mass around 2.2 GeV which is required to reproduce the corresponding (preliminary) angular distribution data from the CBELSA/TAPS Collaboration[13]. We have checked that the (quasi-free neutron) angular distribution data may be reproduced with the $S_{11}$, $P_{11}$, and/or $D_{13}$ resonance with mass value of $m_{\mathrm{R}} \approx 2.2$ GeV and width of about $\Gamma_{\mathrm{R}} \sim$ 50—100 MeV.

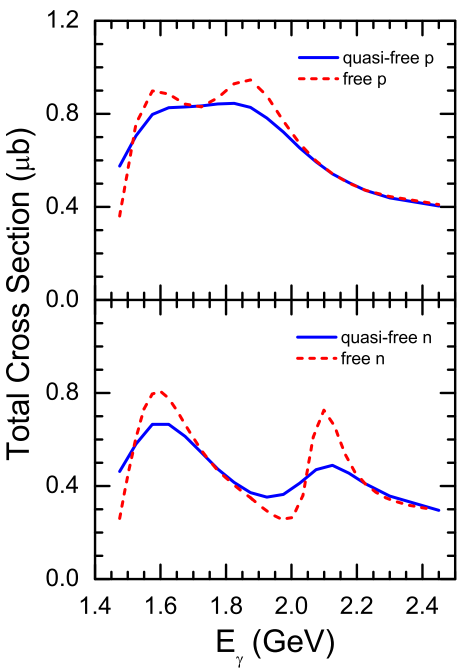


Fig. 3. Predictions for the total cross sections (solid lines) in η′ photoproduction on quasi-free proton (upper panel) and neutron (lower panel). The dashed lines are the corresponding results for the free nucleon targets. See text for further details.

We have also verified that, as in the case of free proton target[18], the beam and target asymmetries are much more sensitive to the values of the model parameters and will help impose much stricter constraints on them once they become available.

### 2.2 NN → η′NN

In this reaction, the dominant production mechanism is found to be the excitation of the $S_{11}$ resonance as can be seen from Fig. 4 (upper panel). The energy dependence exhibited by the pp → η′pp reaction is

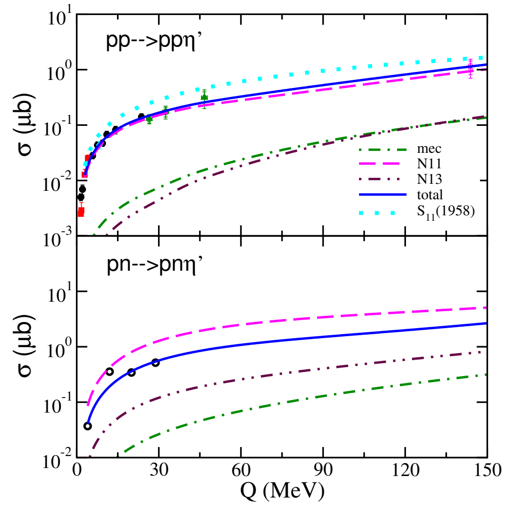


Fig. 4. Results for the total cross sections in pp → η′pp (upper panel) and in pn → η′pn (lower panel) as a function of excess energy $Q$. The dashed line denotes the contribution from the spin-1/2 resonances, while the dash-double-dotted lines from the spin-3/2 resonances. The dashed lines are from the nucleonic current and dash-doted lines from the mesonic current. The dotted line is from the $S_{11}(1958)$ resonance alone. The data are from Refs. [15, 17].

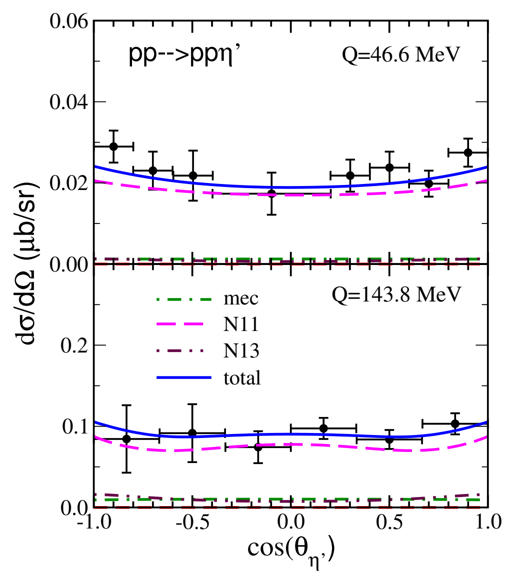


Fig. 5. Results for the η′ angular distributions in pp → η′pp (in the center-of-mass frame) as a function at two excess energies of $Q = 46.6$ and 143.8 MeV. See caption of Fig. 4 for further details. The data are from Ref. [15].

markedly different from that of pp → ηpp. Both the (measured) total and differential cross sections (see, Fig. 5) are rather well reproduced within our model. The present model also reproduces (see the lower panel of Fig. 4) the very preliminary total cross section data (upper limit) for pn → η′pn[17].

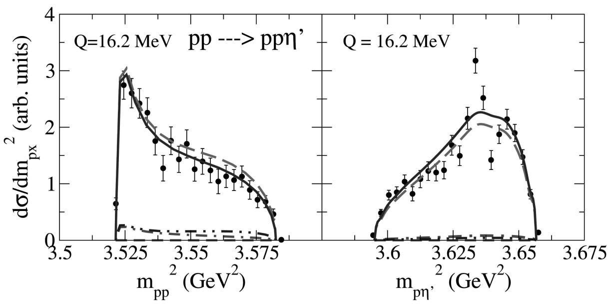


Fig. 6. Results for the pp (left panel) η′p (right panel) invariant mass distributions in pp → η′pp at an excess energy of $Q = 16.2$ MeV. See caption of Fig. 4 for further details. The data are from Ref. [16].

The recent data for pp and pη′ invariant mass distributions[16] are also rather well explained which can be seen from Fig. 6. Here, it is interesting to note that, within the statistical uncertainties, the pp invariant mass distributions for η and η′ productions exhibit similar features. One of the possibilities proposed to explain the measured pp invariant mass distributions in pp → ηpp is the strong ηN FSI in that reaction[21]. We expect, however, that the η′N interaction is much weaker than the ηN interaction.

## 3 Summary

In this work, we have demonstrated that the nucleon resonances are required to describe both the γN → η′N and NN → η′NN reactions. In our model, the $S_{11}$, $P_{11}$, $P_{13}$, and $D_{13}$ resonances can account for the existing data. However, their parameters cannot be determined uniquely from the presently available data, especially, their masses are difficult to be fixed, since the data do not exhibit pronounced bump structures. The exceptions to this may be the two bump structures predicted in photoproduction on free proton at around 2.1 GeV[18] and on quasi-free neutron at around 2.2 GeV, if these are confirmed by experiment. Spin observables in photoproduction (in particular, the beam and target asymmetries) are definitely required to impose more stringent constraints on model parameters.

It should also be mentioned that the existing data on NN → η′NN reaction cannot constrain on the excitation mechanism of the $S_{11}$ resonance. In this connection, data on pn → η′pn and/or pn → η′d will be most needed, for they can disentangle the iso-vector and iso-scalar meson exchange contributions in the excitation of the resonance. In addition, similar to the NN → ηNN process, the analyzing power is also sensitive to the details of the excitation mechanism of the resonance.

## References


1 Capstick S, Isgur N. Phys. Rev. D, 1986, **34**: 2809; Capstick S, Roberts W. ibid., 1993, **47**: 1994; 1994, **49**: 4570; 1998, **57**: 4301; 1998, **58**: 074011

2 Ashman J et al. Phys. Lett. B, 1988, **206**: 364

3 Shore G M, Veneziano G. Nucl. Phys. B, 1992, **381**: 23

4 Hatsuda T. Nucl. Phys. B, 1990, **329**: 376; Efremov A V, Soffer J, Törnqvist N A. Phys. Rev. Lett., 1990, **64**: 1495; Phys. Rev. D, 1991, **44**: 1369

5 Shore G M, Veneziano G. Phys. Lett. B, 1990, **244**: 752

6 Feldmann T. Int. J. Mod. Phys. A, 2000, **15**: 159

7 Okubo S. Phys. Lett., 1963, **5**: 165; Zweig G. CERN Report No. TH412, 1964; Iizuka J. Prog. Theor. Phys. Suppl., 1966, **37-38**: 21.

8 Adams D et al. Phys. Rev. D, 1997, **56**: 5330

9 Altarelli G, Ross G G. Phys. Lett. B, 1988, **212**: 391; Carlitz R D, Collins J C, Müller A H. ibid., 1988, **214**: 229

10 ABBHHM collaboration. Phys. Rev., 1968, **175**: 1669; Nucl. Phys. B, 1976, **108**: 45

11 Plötzke R et al. Phys. Lett. B, 1998, **444**: 555; Barth J et al. Nucl. Phys. A, 2001, **691**: 374c

12 Dugger M et al. Phys. Rev. Lett., 2006, **96**: 062001; ibid., 169905(E)

13 Jaegle I (for CBELSA/TAPS collaboration). in Workshop on the Physics of Excited Nucleons (NSTAR2009), Beijing, April 18-22, 2009; private communication

14 Nakano T (for LEPS/Spring-8 collaboration). in Workshop on the Physics of Excited Nucleons (NSTAR2009), Beijing, April 18-22, 2009; private communication

15 Hibou F et al. Phys. Lett. B, 1998, **438**: 41; Moskal P et al. Phys. Rev. Lett., 1998, **80**: 3202; Moskal P et al. Phys. Lett. B, 2000, **474**: 416; Moskal P et al. ibid. **482**: 356; Balestra F et al. Phys. Lett. B, 2000, **491**: 29; Khoukaz A et al. Eur. Phys. J. A, 2004, **20**: 345

16 Klaja P, Czyzykiewicz R, Moskal P (for COSY-11 collaboration). Proceedings of the Symposium on Meson Physics, Cracow, Poland, Oct. 1-4, 2008, Ed. Moskal P, Acta Phys. Pol. B, 2009, **2**(1): 45; Klaja P. PhD Thesis, 2009

17 Klaja J, Moskal P, Zdebik J (for COSY-11 collaboration). Proceedings of the Symposium on Meson Physics, Cracow, Poland, Oct. 1—4, 2008, Ed. Moskal P, Acta Phys. Pol. B, 2009, **2**(1): 31

18 Nakayama K, Haberzettl H. Phys. Rev. C, 2004, **69**: 065212; ibid., 2006, **73**: 045211

19 Haberzettl H, Nakayama K, Krewald S. Phys. Rev. C, 2006, **74**: 045202

20 Nakayama K, Oh Y, Haberzettl H. arXiv:0803.3169

21 Fix A, Arenhövel H. Phys. Rev. C, 2004, **69** : 014001